

# COMPRESSIVE SENSING OF PARAMETERIZED SHAPES IN IMAGES

Ali Cafer Gurbuz, James H. McClellan, Justin Romberg, and Waymond R. Scott, Jr.

Georgia Institute of Technology  
Atlanta, GA 30332-0250

## ABSTRACT

Compressive Sensing (CS) uses a relatively small number of non-traditional samples in the form of randomized projections to reconstruct sparse or compressible signals. The Hough transform is often used to find lines and other parameterized shapes in images. This paper shows how CS can be used to find parameterized shapes in images, by exploiting sparseness in the Hough transform domain. The utility of the CS-based method is demonstrated for finding lines and circles in noisy images, and then examples of processing GPR and seismic data for tunnel detection are presented.

**Index Terms**— Compressive Sensing, Hough Transform, Shape Detection, Basis pursuit, Convex optimization, line detection

## 1. INTRODUCTION

The problem of detecting parameterized shapes, e.g., lines or circles, arises in many diverse areas of image processing, computer vision and pattern recognition. The Hough Transform (HT) [1] and Generalized Hough Transform (GHT) [2] are well-known methods to detect lines and other parameterized shapes in an image. Both transforms convert the problem of finding the spatially spread patterns in the image space into detecting (sparse) peaks in the parameter space.

The shape-detection problem can be rephrased in terms of the inverse GHT by asking the question: which combination of parameter domain cells represents the image data best? In [3] the line detection problem was posed as an inverse Radon transform<sup>1</sup> problem plus regularization to enhance the detection of lines. If we consider that each cell in the parameter domain corresponds to one image shape, this inverse idea can be used to generate a dictionary of possible shapes. Then basis pursuit [4] can be used to find the best subset of the dictionary elements to represent the image.

Compressive Sensing (CS) [5, 6] can be viewed as a type of basis pursuit framework, but instead of working with the image data, it uses non-traditional samples in the form of randomized projections as measurements. CS has shown that

<sup>1</sup>This work is supported the U.S. Army Research Office under a MURI, contract number DAAD19-02-1-0252.

<sup>1</sup>The Radon transform is the same as the HT for lines

the information in the image is captured in a relatively small number of “random” measurements. Note that our goal is not to reconstruct the image, but rather to detect certain features. For the case of image shape detection, we say that the image is compressible (or sparse) if its GHT contains only a small number of peaks. In the spirit of CS, we solve a linear programming problem to find a sparse set of peaks in the GHT. The locations of these peaks correspond to our detected shape parameters.

One significant property of CS is that the required number of measurements is related to the sparsity of the signal and exact recovery of the signal is guaranteed if the number of measurements greater than the minimum is satisfied. CS shows that in some sense, the best way to collect information about images is by random projections. Imaging devices are being built that take these types of measurements. A new camera architecture that directly acquires random projections of the signal without collecting every pixel has been demonstrated [7]. This paper will talk about using the compressive measurements taken from these devices or some otherway and do feature detection.

This paper deals exclusively with line and circle detections using CS. We show that it is possible to detect the different shapes jointly using the CS framework along with an over-complete representation of shapes. The next section presents the theory of CS shape detection.

## 2. SHAPE DETECTION USING COMPRESSIVE SENSING

The Hough Transform (HT) [1] is the most commonly used algorithm for line detection in images. The HT maps an image into a parameterized domain such that lines in the image correspond to peaks in the parameter domain. An extended version, the Generalized Hough Transform (GHT) [2], maps arbitrary parameterized curves into peaks in the parameter space. The GHT can be formulated as

$$\mathcal{R}(\boldsymbol{\pi})[f(x, y)] = \int f(\varphi_x(\xi, \boldsymbol{\pi}), \varphi_y(\xi, \boldsymbol{\pi}))d\xi \quad (1)$$

where  $\boldsymbol{\pi}$  is an  $p$ -dimensional vector defining the curve parameters and  $\varphi_x(\xi, \boldsymbol{\pi})$  and  $\varphi_y(\xi, \boldsymbol{\pi})$  are functions that define the

specific curve. The GHT transforms from the 2D  $(x, y)$  image space to the  $p$ -D parameter space defined by  $\boldsymbol{\pi}$ .

In order to express the image in terms of an overcomplete dictionary of possible shapes, we must discretize the parameter vector  $\boldsymbol{\pi}$  along each of its  $p$  dimensions. Then we can enumerate a finite set of possible parameter vectors  $\mathcal{P} = \{\boldsymbol{\pi}_1, \boldsymbol{\pi}_2, \dots, \boldsymbol{\pi}_N\}$ , where  $N$  depends on the discretization that we pick. Finally, we define the vector  $\boldsymbol{p}$  to be an indicator and weight function, i.e., the  $k^{\text{th}}$  element of  $\boldsymbol{p}$  is nonzero if we want to select (and weight) parameter  $\boldsymbol{\pi}_k$ .

Now we are ready to create the overcomplete dictionary by using the inverse relation between the parameter space selector  $\boldsymbol{p}$  and the image  $\boldsymbol{f}$ , which can be written as

$$\boldsymbol{f} = \boldsymbol{H}\boldsymbol{p} \quad (2)$$

where  $\boldsymbol{H}$  is, in some sense, an inverse GHT operator. The  $L \times L$  image must be concatenated into a length- $L^2$  vector  $\boldsymbol{f}$ . Each column of  $\boldsymbol{H}$  is one possible parameterized shape in the image domain, i.e., the  $k^{\text{th}}$  column of  $\boldsymbol{H}$  corresponds to the shape with parameters  $\boldsymbol{\pi}_k$ . The matrix  $\boldsymbol{H}$  is called the sparsity basis because we can represent the image using a small number of columns from  $\boldsymbol{H}$ . We say that the image is  $K$ -sparse if its GHT has no more than  $K$  nonzero peaks, or, equivalently, the vector  $\boldsymbol{p}$  has no more than  $K$  nonzero elements.

Consider our  $K$ -sparse signal  $\boldsymbol{p}$  of length  $N$  as our parameter space signal where the image  $\boldsymbol{f}$  is represented as in (2). In CS rather than sampling all the pixels in the image  $\boldsymbol{f}$  we measure linear projections of  $\boldsymbol{f}$  into a second set of basis vectors  $\boldsymbol{\phi}_m$ ,  $m = 1, 2, \dots, M$ . Here many fewer samples than the size of  $\boldsymbol{p}$  are taken,  $M \ll N$ . In matrix notation we measure

$$\boldsymbol{y} = \boldsymbol{\Phi}\boldsymbol{f} = \boldsymbol{\Phi}\boldsymbol{H}\boldsymbol{p} \quad (3)$$

The result of CS theory is that sparse parameter domain signal  $\boldsymbol{p}$  can be recovered exactly from

$$M = C(\mu^2(\boldsymbol{\Phi}, \boldsymbol{H}) \log N) K \quad (4)$$

CS measurements  $\boldsymbol{y}$  by solving an  $\ell_1$  minimization problem as

$$\hat{\boldsymbol{p}} = \operatorname{argmin} \|\boldsymbol{p}\|_1 \quad \text{s.t.} \quad \boldsymbol{y} = \boldsymbol{\Phi}\boldsymbol{H}\boldsymbol{p} \quad (5)$$

with overwhelming probability [6], where  $\mu(\boldsymbol{\Phi}, \boldsymbol{H})$  is the coherence between  $\boldsymbol{\Phi}$  and  $\boldsymbol{H}$  defined as in [6]

The optimization problem in (5) is valid for the noiseless case. For noisy compressive measurements in the form

$$\boldsymbol{y} = \boldsymbol{A}\boldsymbol{p} + \boldsymbol{z} \quad \boldsymbol{z}_k \sim \mathcal{N}(0, \sigma^2) \quad (6)$$

where  $\boldsymbol{A} = \boldsymbol{\Phi}\boldsymbol{H}$ , the following optimization problems will recover the sparse  $\boldsymbol{p}$ . The Dantzig Selector [8, 9] recovers the sparse  $\boldsymbol{p}$ . Instead of (5) the following convex optimization problem is solved.

$$\min \|\boldsymbol{p}\|_1 \quad \text{s.t.} \quad \|\boldsymbol{A}^T(\boldsymbol{y} - \boldsymbol{A}\boldsymbol{p})\|_\infty < \lambda_N \sigma \quad (7)$$

Equation (7) is called the Dantzig selector [8] and selecting  $\lambda_N = \sqrt{2 \log N}$  makes the true  $\boldsymbol{p}$  feasible with high probability. Another possible solution comes from constraining the  $\ell_2$ -norm of the error in measurements to be less than some  $\epsilon$ .

$$\min \|\boldsymbol{p}\|_1 \quad \text{s.t.} \quad \|\boldsymbol{y} - \boldsymbol{A}\boldsymbol{p}\|_2 < \epsilon \quad (8)$$

Greedy algorithms like Matching Pursuit (MP) and orthogonal matching pursuit (OMP) [10] are also used to find a sparse description for the measured data. However, only OMP is guaranteed to converge to a sparse solution [11]. The parameters in (7) and (8) need to be estimated or properly selected. Cross validation [11] is shown to be a good solution about selecting the parameters or stopping conditions. Results from the above stated algorithms are shown in Section 3.

The optimization problems in (5) and (7) can be solved by linear programming techniques, while (8) is a second-order cone program. Since all of these minimize convex functionals, a global optimum is guaranteed. In [3] a non-convex functional is used as a regularizer, but the resulting stationary point is not necessarily the global minimum.

### 3. RESULTS

#### 3.1. Detecting Linear Structures

An important application of shape detection is detecting linear structures in images. Figure 1 shows a noisy gray-scale image with 3 lines having the parameters  $\rho = [-3, 21, -27]$  and  $\theta = [33, 132, 153]$  degrees. The image is  $50 \times 50$ , i.e., 2500 pixel values. For detecting lines in the image only 400 projections (compressive samples) of the image with random Gaussian vectors are used. The compressive samples,  $\boldsymbol{y}$ , of the noisy image are shown in Fig. 1(c). We assume that these samples are the only information we have about the image and our goal is to find the linear structures in the image. One possible reconstruction is to find the parameter space image which has minimum  $\ell_2$ -norm that satisfies the compressive measurements. The result is the parameter space image shown in Fig. 1(d). This solution is a feasible solution because it satisfies the constraint  $\boldsymbol{y} = \boldsymbol{A}\boldsymbol{p}$ , but this parameter space image doesn't give any reliable information about possible line locations.

If the problem stated in (7) is solved, the parameter space image shown in Fig. 1(f) is obtained. It can be seen that the resultant image is sparse with 3 peaks corresponding to the true line parameters. If we had the information about all the pixels of the image and had applied the standard Hough transform to the original image we would obtain the image in Fig. 1(e). Even though the Hough transform image shows 3 significant peaks, it is more noisy, and it requires  $L^2$  measurements (all the pixels in the image).

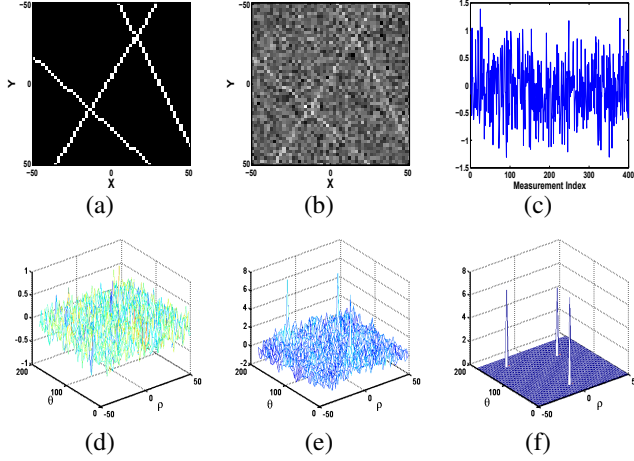


**Fig. 1.** (a) Image showing true line locations, (b) Noisy image with additive white Gaussian noise ( $\sigma = 0.5$ ), (c) Compressive measurements, (d) Parameter space image obtained with  $\ell_2$ -norm minimization, (e) Hough Transform using all the image pixels, (f)  $\ell_1$ -minimization using the Dantzig Selector.

### 3.2. Joint Detection of Circles and Lines

The standard Hough Transform calculates the votes for each parameter space value. To detect circles in an image a HT with circle parametrization should be taken and the peaks in the parameter space should be searched. The same procedure should be repeated for the same image for detecting lines with creating a separate parameter space using line parametrization. Having different shapes in the image might be problematic since line pixels will be voted for varying circle parameters or vice versa. But the proposed procedure for detecting shapes allows joint detection of different shapes in the image. We can relate the image  $f$  to the parameter space of lines and

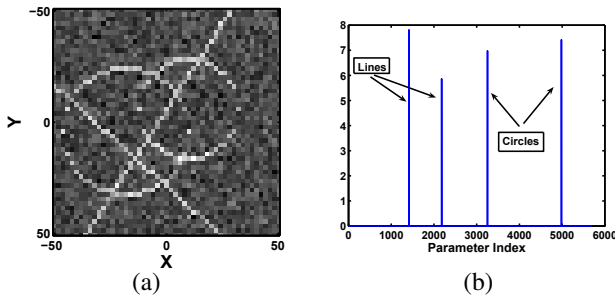


**Fig. 2.** (a) Noisy image with additive white Gaussian noise ( $\sigma = 0.2$ ), (b)  $\ell_1$ -minimization by Dantzig Selector.

circles using an overcomplete dictionary of shapes.

$$f = [H_l \ H_c] \begin{bmatrix} p_l \\ p_c \end{bmatrix} \Rightarrow y = \Phi f \quad (9)$$

where  $H_l$  and  $H_c$  are the sparsity basis and  $p_l$  and  $p_c$  are the parameter spaces for line and circle respectively. The sparse parameter space  $(p_l \ p_c)$  can be reconstructed using one of the convex optimization problems presented in Section 2 from compressive measurements  $y$ .

Figure 2 shows a noisy gray-scale image containing two circles with centers at  $(10, -6)$  and  $(-18, 4)$  and radii 22 and 28, respectively, and two lines with parameters  $\rho = [-3, 21]$  and  $\theta = [33, 132]$ . Only 500 compressive measurements are used. The joint optimization problem in (7) is solved and the resultant joint parameter space is shown in Fig. 2(d).

### 3.3. Detecting Buried Pipes in Seismic or GPR Images

One possible application of shape detection is finding buried structures in subsurface images. Figure 3(a) shows backprojected seismic surface energy image taken over a buried pipe [12]. The standard HT of the image is shown in Fig. 3(b). The two peaks in Hough domain corresponding to the two linear structures in the image can be observed. For detect-

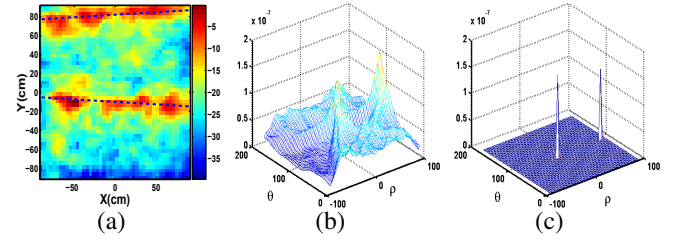


**Fig. 3.** (a) Experimental Backprojected Seismic Image, (b) Hough Transform of the image, (c) Parameter space image using OMP with cross validation algorithm.

ing lines in the image only 400 compressive samples of the image with random Gaussian vectors are used. The parameter space is reconstructed using OMP algorithm with cross validation [11]. From the 400 measurements 350 are used for OMP and 50 measurements are used for cross validation. The OMP algorithm is stopped when the norm of the error,  $\|y_{cv} - Ap\|_2$  starts to increase. Here  $y_{cv}$  are cross validation measurements and  $p$  is the parameter space at the current iteration. This will reduce the overfitting of OMP to explain some portion of the noise or underfitting which is not to fully reconstruct  $p$ . The result of the applied algorithm is shown in Fig. 3(c). A much cleaner and sparser image than the standard HT is obtained with two peaks only. This way there is no need to search for local maximums in HT domain to detect the lines. The parameters of the detected two peaks are  $\rho = [-10, 82]$  and  $\theta = [87, 93]$ . The corresponding lines are drawn on the original image in Fig. 3(a).

### 3.4. Performance in Noise

To analyze the performance of the algorithm with varying noise levels the algorithm is applied to images with SNRs from  $-25$  dB to  $10$  dB. At each SNR level one random linear structure is corrupted by WGN with zero mean and corresponding variance. The Dantzig selector is used to detect the linear structure parameters. This procedure is repeated 50 times with random initialization of noise at each time and correct detections are counted. The detection ratio vs. SNR plot for different compressive measurements are shown in Fig. 4(a).

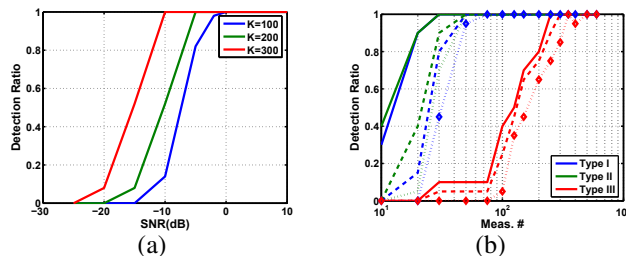


**Fig. 4.** (a) Detection ratio vs. SNR , (b) Detection ratio vs. measurement number for varying types of random matrices (Solid, dash and diamond marked dotted lines correspond to 1, 2, and 3 targets respectively).

It can be observed that proposed algorithm detects shapes in very noisy images using a small number of measurements and increasing the number of measurements increases the detection ratio for the same SNR value.

### 3.5. Test on Number of Compressive Measurements

For exact recovery of  $K$ -sparse signals the required number of compressive measurements is given by (4). This quantity depends on the mutual coherence between the sparsity basis and the random projection matrix used. Here three different types of random matrices are tested (see Fig. 4(b)). The entries of the Type I random matrix are drawn from  $\mathcal{N}(0, 1)$ . The Type II random matrix has random  $\pm 1$  entries with probability of  $1/2$ , and the Type III random matrix is constructed by randomly selecting some rows of an identity matrix of size  $N$  which amounts to measuring random pixels of the image at each measurement. Each matrix is normalized to have unit norm rows.

The average mutual coherence between the random matrices and the sparsity basis for a line are  $\mu_1 = 5.2751$ ,  $\mu_2 = 5.0059$  and  $\mu_3 = 12.7500$  for Type I, II and III random matrices respectively. This means that the required number of compressive measurements to detect a shape will be similar if Type I or II matrices are used. Using Type III matrix will require approximately 6.5 times more compressive measurements for the same detection capability.

A Monte-Carlo simulation is done to test the required number of compressive measurements for each random matrix type. Each random matrix is tested with 1, 2 and 3 shapes in the image. Figure 4(b) shows detection ratio for varying measurement numbers. It can be observed that the required compressive measurement number increases for all types of random matrices when used with an increasing number of targets. While Type I and II random matrices require similar number of measurements, Type III random matrices require many more measurements to detect the same number of targets as expected from the mutual coherence given above.

## 4. REFERENCES

- [1] P. V. C. Hough, "A Method and Means for Recognizing Complex Patterns," in *US Patent 3069654*, Dec. 1962.
- [2] P. Toft, "Using the generalized Radon transform for detection of curves in noisy images," in *ICASSP-2006*, 1996, vol. 4, pp. 2219–2222.
- [3] N. Aggarwal and W. C. Karl, "Line detection in images through Regularized Hough Transform," *IEEE Trans. on Image Processing*, vol. 15, pp. 582–590, 2006.
- [4] S. S. Chen, D. L. Donoho, and M. A. Saunders, "Atomic decomposition by basis pursuit," *SIAM J. Sci. Comput.*, vol. 20, pp. 33–61, 1999.
- [5] D. L. Donoho, "Compressive sensing," *IEEE Trans. on Information Theory*, vol. 52(4), pp. 1289–1306, 2006.
- [6] E. J. Candes, J. Romberg, and T. Tao, "Robust uncertainty principles: Exact signal reconstruction from highly incomplete frequency information," *IEEE Trans. on Information Theory*, vol. 52, pp. 489–509, 2006.
- [7] D. Takhar et.al, "A new compressive imaging camera architecture using optical-domain compression," in *Proc. Comp. Imaging IV at SPIE Electronic Imaging*, 2006.
- [8] E. Candes and T. Tao, "The Dantzig Selector: Statistical estimation when  $p$  is much larger than  $n$ ," *To appear in Annals of Statistics*.
- [9] E. Candès, J. Romberg, and T. Tao, "Stable signal recovery from incomplete and inaccurate measurements," *Comm. on Pure and Applied Math.*, vol. 59, no. 8, pp. 1207–1223, 2006.
- [10] S. Mallat and Z. Zhang, "Matching pursuits with time-frequency dictionaries," *IEEE Trans. Signal Processing*, vol. 41, 1993.
- [11] P. Boufounos, M.F. Duarte, and R. Baraniuk, "Sparse signal reconstruction from noisy compressive measurements using cross validation," in *Proc. IEEE Workshop on SSP*, August 2007.
- [12] W. R. Scott, Jr., T. Counts, G. D. Larson, A. C. Gurbuz, and J. H. McClellan, "Combined ground penetrating radar and seismic system for detecting tunnels," in *IEEE IGARSS*, July 2006, pp. 1232–1235.